3B2v7.51c GML4.3.1 CAGEO : 1200 Prod.Type:COM pp.1–19(col.fig.:NIL) ED:Rohini PAGN: Murthy.N SCAN: Vinod

ARTICLE IN PRESS

PERGAMON

Computers & Geosciences ▮ (▮▮▮▮) ▮▮▮–▮▮▮

COMPUTERS & GEOSCIENCES

www.elsevier.com/locate/cageo

Modeling Np and Pu transport with a surface complexation model and spatially variant sorption capacities: implications for reactive transport modeling and performance assessments of nuclear waste disposal sites

Pierre D. Glynn

US Geological Survey, 436 National Center, Reston, VA 20191, USA

Received 20 May 2002; received in revised form 23 August 2002; accepted 30 September 2002

Abstract

One-dimensional (1D) geochemical transport modeling is used to demonstrate the effects of speciation and sorption reactions on the ground-water transport of Np and Pu, two redox-sensitive elements. Earlier 1D simulations considered the kinetically limited dissolution of calcite and its effect on ion-exchange reactions (involving ^{90}Sr, Ca, Na, Mg and K), and documented the spatial variation of a ^{90}Sr partition coefficient under both transient and steady-state chemical conditions. In contrast, the simulations presented here assume local equilibrium for all reactions, and consider sorption on constant potential, rather than constant charge, surfaces. Reardon's (1981) seminal findings on the spatial and temporal variability of partitioning (of ^{90}Sr) are reexamined and found partially caused by his assumption of a kinetically limited reaction.

In the present work, sorption is assumed the predominant retardation process controlling Pu and Np transport, and is simulated using a diffuse-double-layer-surface-complexation (DDLSC) model. Transport simulations consider the infiltration of Np- and Pu-contaminated waters into an initially uncontaminated environment, followed by the cleanup of the resultant contamination with uncontaminated water. Simulations are conducted using different spatial distributions of sorption capacities (with the same total potential sorption capacity, but with different variances and spatial correlation structures). Results obtained differ markedly from those that would be obtained in transport simulations using constant K_d, Langmuir or Freundlich sorption models. When possible, simulation results (breakthrough curves) are fitted to a constant K_d advection–dispersion transport model and compared. Functional differences often are great enough that they prevent a meaningful fit of the simulation results with a constant K_d (or even a Langmuir or Freundlich) model, even in the case of Np, a weakly sorbed radionuclide under the simulation conditions. Functional behaviors that cannot be fit include concentration trend reversals and radionuclide desorption spikes. Other simulation results are fit successfully but the fitted parameters (K_d and dispersivity) vary significantly depending on simulation conditions (e.g. "infiltration" vs. "cleanup" conditions). Notably, an increase in the variance of the specified sorption capacities results in a marked increase in the dispersion of the radionuclides.

The results presented have implications for the simulation of radionuclide migration in performance assessments of nuclear waste-disposal sites, for the future monitoring of those sites, and more generally for modeling contaminant transport in ground-water environments.

Keywords: Radionuclide transport; K_d; Langmuir; Freundlich; Geochemical modeling; Linear partition coefficient

E-mail address: pglynn@usgs.gov (P.D. Glynn).

0098-3004/03/$ - see front matter © 2003 Published by Elsevier Science Ltd.
doi:10.1016/S0098-3004(03)00009-8

1. Introduction and Background

1.1. Partition coefficients used in reactive transport modeling

Computer codes used to model the reactive transport of ground-water contaminants (e.g. for performance assessments of nuclear waste-disposal sites) often assume that the reactions governing the retardation of a particular contaminant or radionuclide can be described by a simple partitioning constant, K_d. This constant is assumed to account for all the reversible sorption processes affecting transport of the contaminant. The most frequent definition of K_d for use in porous media environments is

$$K_d = \frac{q}{c}, \tag{1}$$

where q represents the amount sorbed, per unit weight of solid, and c represents the amount in solution, per unit volume of solution. K_d values are expressed typically in ml/g or in l/kg. Most often, K_d values are derived from "batch" experiments where a given mass of solid is put in contact with an aqueous solution containing a specific contaminant. Another way of measuring K_d values is through column experiments that measure the retardation R of a reactive contaminant relative to the transport of a "chemically conservative" constituent. The dimensionless factor R can be related to the K_d value by

$$R = 1 + \left(\frac{1-n}{n}\right)\rho_s K_d = 1 + \frac{\rho_b}{n}K_d, \tag{2}$$

where n is the porosity of the medium, ρ_s is the solid density, and ρ_b is the bulk density of the medium. Given this definition, K_d coefficients can be incorporated in the advection–dispersion equation used to describe contaminant transport in ground-water systems by multiplying the advective and dispersive terms of the equation by the retardation factor, R.

Other slightly different definitions of constant partitioning factors are also sometimes used. For example, for transport in fractured-rock systems, a K_f value is sometimes defined as

$$K_f = \frac{s}{c}, \tag{3}$$

where s is now the amount sorbed, per unit surface area of fracture. As a result, K_f has units of volume per surface area (e.g. l/m^2), or simply of length (m). In this situation, the dimensionless retardation factor R can be related to K_f by

$$R = 1 + 2\frac{K_f}{b}, \tag{4}$$

where b is the fracture aperture.

Alternatively, the partitioning constant can be expressed as an amount sorbed per volume of contacting water divided by the concentration in solution, or, as done here, as the dimensionless "partitioning ratio", K_r, the number of moles of contaminant sorbed per kg of contacting H_2O, $m_{i,\mathrm{sorbed}}$ divided by the molality of the contaminant in solution, $m_{i,\mathrm{aq}}$:

$$K_r = \frac{m_{i,\mathrm{sorbed}}}{m_{i,\mathrm{aq}}}. \tag{5}$$

Following the above definition, the retardation of a contaminant due to sorption is simply

$$R = 1 + K_r. \tag{6}$$

Despite the differences in definitions, the sorption model expressed by either Eqs. (1), (3) or (5), will be referred to in this paper as the "K_d approach", if the partitioning ratio, K_d, K_f or K_r, is assumed constant over the transport domain and time scale considered.

1.2. Advantages and limitations of the K_d approach

The mathematical simplicity of the K_d approach is its primary advantage. Any computer code used to simulate the transport of a conservative, non-reactive component can be easily modified to solve the transport equation for a reactive "retarded" component if the partitioning coefficient expressed by Eqs. (1), (3) or (5), is assumed constant. The use of the K_d approach in transport codes ignores the multitude of aqueous, surface and solid-phase reactions that may be occurring in the ground-water environment, but has the advantage of not having to depend on often highly uncertain thermodynamic constants.

Experimental determinations of K_d values are also relatively easy to perform, particularly through "batch tests". Despite prolific K_d measurements, however, conditions that can affect the measurements often are insufficiently controlled during the experiments and are rarely described with adequate detail; consequently K_d values obtained often cannot be used to predict partitioning under different sets of conditions. Experimental conditions that can affect K_d measurements include pH, redox speciation, dissolved gas and solute concentrations, temperature and pressure, physical, chemical and mineralogical characteristics of available sorbing surfaces, stirring rates and/or flow rates.

K_d measurement or estimation techniques, whether based on laboratory measurements or field observations, rarely consider explicitly the chemical and physical processes that may be responsible for the partitioning of a constituent between mobile and immobile phases. The partitioning generally is considered to involve a reversible sorption process, even though the constituent of interest may also undergo partitioning due to (1) chemical processes such as solid-phase precipitation, partitioning into a solid-solution phase and volatilization, or (2) physico-chemical processes, such as diffusion into immobile-fluid zones.

Despite the assumption that K_d's account for partitioning caused by sorption of a constituent onto mineral surfaces, K_d values commonly are normalized to a given mass of solid material rather than to a given solid-surface area. Experimenters typically ignore the effect of surface to mass ratios, or grain size, on K_d determinations. They also often ignore the effects that rock crushing may have on K_d determinations. The sorptive properties of a freshly fractured rock surface can be expected to differ markedly from those of an ancient, naturally weathered surface. Freshly fractured surfaces are full of crystal dislocations and time-dependent, high-energy sites created by the crushing process. They also do not contain any significant abundance of secondary minerals generated by the natural weathering of primary minerals. Sorption of a constituent on the fracture surfaces of granitic or basaltic rock is often "predicted" through the use of K_d values determined from experiments performed on the crushed rock. K_d determinations rarely consider the mineralogy or physical properties of the sorbing materials.

The K_d approach inherently assumes that the sorbing surfaces contain an infinite number of potential sorption sites, all with the same thermodynamic sorbing potential: if the aqueous concentration of a constituent is increased by a given factor, the amount of sorbed constituent is assumed to increase by the same factor. Observations generally show instead that as aqueous concentrations increase, the ratio of sorbed to aqueous concentrations tends to decrease, rather than remain constant. As a result, many computer codes that simulate transport of ground-water contaminants now offer the possibility of simulating sorption processes using a Langmuir isotherm or Freundlich isotherm approach, instead of the linear isotherm or K_d approach. Both the Langmuir and Freundlich isotherms can simulate a decreasing ratio of sorbed to aqueous concentration with increasing aqueous concentrations. The Langmuir isotherm exhibits the realistic property of simulating a maximum number of sorption sites. The Freundlich isotherm does not have this capability but, in contrast to the Langmuir isotherm, it has the capability of simulating an *increasing* ratio of sorbed to aqueous concentration with an increase in aqueous concentrations. Although relatively uncommon, this behavior is sometimes exhibited by constituents undergoing ion exchange, until the constituent fills all exchange sites. The situation occurs in the presence of another constituent that shows preferential exchange (given equal aqueous concentrations of both constituents).

The sorption models mentioned above (the linear isotherm or "K_d" approach, the Freundlich isotherm, and the Langmuir isotherm) apply only to single components. The models do not consider the effect of competitive sorption by other components of the aqueous solution. The models also do not account for the aqueous speciation of the component of interest. Although ignoring outer-sphere aqueous species (ion pairs) may be acceptable, ignoring inner-sphere species (complexes), which have stronger chemical bonds, is probably not. Even though specific aqueous species of a given component may be much more strongly sorbed than other species of that same component, the K_d, Langmuir and Freundlich models only consider the total aqueous concentrations of the component, and, therefore, ignore the thermodynamic properties of its constituent aqueous species. This major limitation is particularly problematic for elements with multiple oxidation states (such as Pu, Np and many actinides), given that different oxidation states commonly have extremely different aqueous stabilities and sorption affinities.

The K_d, Langmuir and Freundlich models also ignore the speciation of the sorbing surface. Although certain minerals (such as clays and zeolites) have a relatively fixed number of sorption sites, i.e. a constant charge, regardless of the composition and pH of the contacting solution, other minerals have surface properties (such as the number of surface sites with a particular charge) that vary strongly as a function of the pH and aqueous composition of the contacting solution. Ion exchange models are typically used to describe "constant charge" surfaces, whereas surface-complexation models are commonly used to describe "constant potential" surfaces in which the number of potential sorption sites is constant, but the distribution of charges (negative, positive and neutral) amongst those sites is not, and depends on the composition and pH of the contacting aqueous solution.

1.3. *Reardon's (1981) numerical investigation of the K_d concept*

The K_d approach may adequately describe contaminant migration and reversible sorption in ground-water systems in which the contaminated and yet-to-be-contaminated aquifer domains each have uniform mineralogical and chemical compositions, which remain uniform through the time scale of interest (although one domain may be expanding at the expense of the other). In general, the reactive sorption of the contaminant of interest must also be adequately described by the local equilibrium assumption (LEA): the reaction rate of the contaminant in a representative unit volume of aquifer must be fast relative to its transport through that volume. If this is not the case, the system will not be described by two chemically and mineralogically uniform regions.

In a seminal paper, Reardon (1981) demonstrated that the K_d approach could not properly describe contaminant migration in ground-water systems undergoing dynamic chemical evolution, and could not even

properly describe contaminant migration in systems that were at chemical steady state. In systems at chemical steady state, K_d values may vary spatially, but will be constant through time at any given point in the system. Most contaminated ground-water systems are not at chemical steady state and instead can be best described as dynamically evolving systems, in which K_d values (or equivalent partitioning coefficients) will vary not only spatially but also through the time scale of interest.

Reardon (1981) described the results of a one-dimensional (1D) reactive transport simulation in which ^{90}Sr, the contaminant of interest, underwent ion-exchange reactions with Ca, Na, K and Mg on an inert clay. The concentration of Ca in the solution and consequently the concentrations of all the other cations considered were affected by the dissolution of calcite, which was described by a kinetic model, rather than by the LEA. The LEA was used, however, to describe the ion-exchange reactions. At chemical steady state, the dimensionless K_r values for ^{90}Sr varied throughout the 1D system by approximately a factor of two, as a function of the saturation index of calcite (cf. Fig. 1). Because the dissolution of calcite was kinetically limited, calcite saturation was only reached approximately midway through the column. Should the calcite have reacted sufficiently fast for the LEA to apply, and should initial calcite concentrations have been sufficiently large not to be depleted anywhere in the system during the time scale of interest, K_r (and equivalently K_d) values would have been uniform throughout the column. This conclusion is supported by the 1D geochemical-transport simulations conducted by Glynn and Brown (1996) and Glynn et al. (1991). Each simulation, part of a sensitivity analysis of reactive transport at a site of acidic heavy-metal contamination near Globe, Arizona, considered a different set of mineral, gas and ion-exchange reactions generally assumed to be at local equilibrium. In each simulation, the movement of various reaction fronts was found to be nearly constant in initially uniform columns (although calculated retardation factors did depend on the reactions considered in any given simulation).

There are many commonly occurring chemical reactions that can have significant effects on ground-water chemical evolution and for which applying the LEA might be inappropriate. These most notably include the oxidation of dissolved or particulate organic matter, other redox reactions (such as the reaction of dissolved oxygen with Fe(II)-containing biotite or chlorite), the dissolution of primary silicate minerals and the formation of secondary silicates. As Reardon (1981) demonstrated, partitioning coefficients (K_d values) affected by these kinetically limited reactions could be expected to vary spatially, even at chemical steady-state, in the region where the sorption-controlling chemical characteristics of the waters also varied.

Fig. 2 shows how the K_r values varied in Reardon's (1981) simulations, prior to attainment of chemical steady state, that is under conditions of dynamic chemical evolution. Under these conditions, K_r values can be seen to vary spatially and temporally by close to an order of magnitude. K_d values would vary in a similar fashion.

1.4. Objectives

The objectives of this paper are to extend the work of Reardon (1981); specifically, to investigate the functional differences that may be obtained by using a surface-complexation and aqueous speciation model, rather than a constant K_d model, and to describe contaminant sorption in 1D transport simulations.

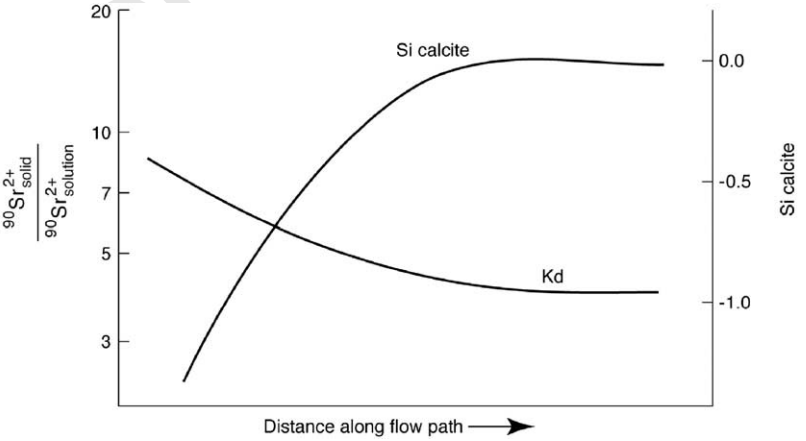

Fig. 1. Variation of calcite saturation indices ($SI_{calcite}$) and ^{90}Sr partitioning (K_d) between solution and an ion exchange phase in a 1D column at chemical steady state (from Reardon, 1981). Reprinted by permission of Ground Water. Copyright 1981.

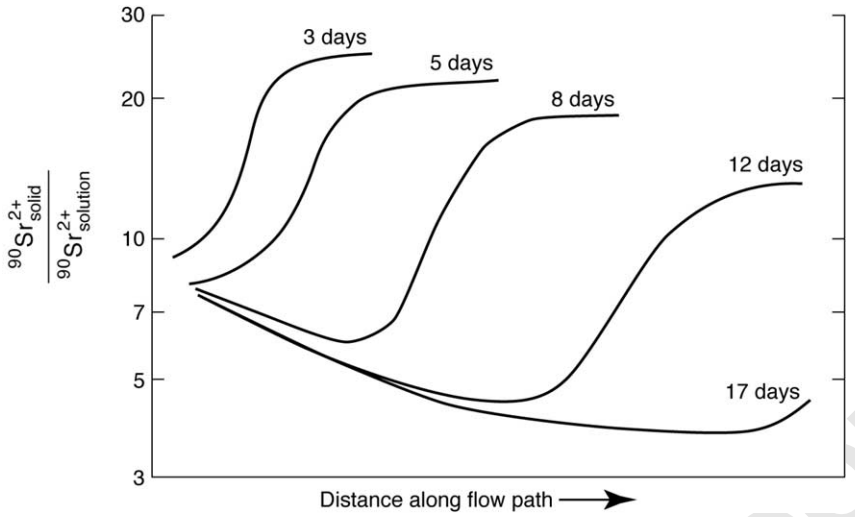

Fig. 2. Temporal and spatial changes in ^{90}Sr partitioning (K_d) between solution and an ion-exchange phase in a dynamically evolving ground-water system. After 17 days of transport time, system is near chemical steady state (from Reardon, 1981). Reprinted by permission of Ground Water. Copyright 1981.

Additionally, the effects of using spatially heterogeneous distributions of potential sorption capacities are also considered. Although specific contaminants (Pu and Np), specific waters (from the Äspö site in Sweden) and a specific scenario are considered in the present simulations, the investigation is meant to be as generic as possible.

2. Speciation-based approach to sorption modeling

2.1. Numerical modeling capabilities, uncertainties and limitations

In contrast to computer codes that use the K_d concept and simulate the transport of only a single component, several multi-species reactive transport codes currently offer the possibility of accounting for a wide variety of chemical reactions that can affect the transport of contaminants. These codes are associated with a thermodynamic database that is used to calculate the equilibrium state of the waters and contacting surfaces, minerals, and gases in the ground-water system as a function of both time and space. Some codes have the additional capability of simulating the kinetic restrictions that may prevent equilibrium states from being reached instantaneously. The advantage of multi-species reactive transport codes is that in addition to the possibility of simulating more realistically the numerous complex chemical processes that may affect the behavior and fate of contaminants, the codes are based on a set of thermodynamic constants, that in theory, at a fixed temperature and pressure, should be independent of actual field conditions.

Typically, thermodynamic constants are determined in well-controlled laboratory experiments. Although thermodynamic data describing the reaction of major cations and anions commonly present in natural waters are relatively well known, at least for reactions that are sufficiently fast to have been successfully simulated under laboratory time scales, large knowledge gaps and uncertainties exist concerning the thermodynamic properties and behavior of elements and molecular species that are of concern in contaminant transport studies. The thermodynamic properties and behavior of radionuclides are not particularly well known. This is true even for elements such as Pu, Np, Am, Tc and U, which are often of high concern in performance assessments of nuclear waste disposal sites, and are a focus of international thermodynamic database generation and refinement efforts such as the Thermochemical Data Base project (web reference: http://www.nea.fr/html/dbtdb/cgi-bin/tdbdocproc.cgi) conducted under the auspices of the Nuclear Energy Agency (NEA) of the Organization for Economic Cooperation and Development (OECD).

Additionally, the thermodynamic properties of mineral surfaces are difficult to characterize in the field and even in the lab. Many uncertainties exist regarding the thermodynamic behavior of "mixtures" of surfaces and the effects caused by the aging, poisoning, and recrystallization of mineral surfaces. Discriminating between different processes, such as uptake of a contaminant by sorption or by solid-solution formation/recrystallization, also may be difficult. In addition, uncertainties arise because the sorption behavior of complex mineral assemblages, present in most field environments, is not well known. Transport simulation

models often ignore such assemblages, and reduce complex and interdependent sets of sorption properties to those of a single surface type. Davis et al. (1998) discuss the benefits and limitations of this "generalized composite" approach, and compare it to the "component additivity" approach. This latter approach uses thermodynamic constants that may be more generally applicable to a variety of field settings, but its application requires appreciably more data because *all* the available sorbing surfaces in a field situation need to be characterized.

The simulation of chemical reactions under conditions of chemical equilibrium is also often not relevant to field conditions because of kinetic limitations in the reactions of interest. Knowledge of reaction kinetics is substantially more limited, and more dependent on actual field conditions, than knowledge of thermodynamic properties. Any attempt to determine reaction kinetics from field observations is constrained by difficulties in gaining sufficiently detailed knowledge of the physical properties of a ground-water system.

Simulations conducted with multi-species reactive transport codes can require inordinate amounts of computer time to obtain results, particularly if 2D or 3D simulations are conducted. Unfortunately, sensitivity analyses, for which simulations must be run numerous times while changing only a few parameters at a time, are one of the essential uses of full-featured computer codes. Consequently, any increase in simulation complexity generally requires an even more significant increase in the number of simulation runs, so as to truly understand the results obtained. Although computer time restrictions are easing, the desire to increase the complexity of contaminant transport simulations to the maximum limit of computer capabilities is always present, often to the detriment of gaining a better understanding of contaminant transport in the ground-water system being investigated.

Given these uncertainties and limitations, simple models that successfully simulate the essential properties of contaminant transport and reaction have an undeniable appeal. Because of its many limitations, however, the K_d approach may be too restrictive in simulating reactive transport.

2.2. Field environment uncertainties in modeling radionuclide sorption and retardation: the Fennoscandian ground-water environment

The simulations presented in this paper were prepared in an effort to help the Swedish Nuclear Power Inspectorate (SKI) assess the advantages and limitations of using a constant K_d linear sorption model in numerical simulations of radionuclide transport, such as are often conducted in performance assessments of nuclear waste-disposal sites. The simple simulations presented here consider a few chemical and mineralogical aspects of the present Fennoscandian ground-water environment, particularly as found at 500 m depth near the Äspö Hard Rock Laboratory (HRL) on the eastern coast of southern Sweden. The simulations consider some aspects of the potential evolution of this environment thousands to ten thousands of years into the future. The chemical, mineralogical, hydrological, and geological characteristics of the Äspö site and the consideration of its potential evolution are discussed in several SKI reports as part of the SITE-94 project (SKI SITE-94, 1996; Glynn and Voss, 1999).

Despite an intense data gathering effort by Swedish, Finnish and other national government agencies, particularly with respect to the Äspö HRL site, simulations of radionuclide transport in Fennoscandian ground waters conducted for performance assessments related to nuclear waste disposal are hampered by a lack of sufficiently detailed knowledge of the geology, hydrology, chemistry, and mineralogy of the highly heterogeneous crystalline rock environments. In addition, performance assessments often require consideration of the possible evolution of a ground-water environment over thousands to hundreds of thousands of years or more; any analysis of such evolution carries many additional uncertainties. In performance assessments, the far-field environment, i.e. the natural rock environment surrounding a disposal site, typically is considered an additional natural barrier to radionuclide migration, separate from the engineered barriers of the near-field environment, and therefore its potential evolution and alteration must be taken into account.

The chemistry of the waters in the near-field environment (the canister(s) and surrounding engineered barriers) of a nuclear waste-disposal site can be expected to differ significantly from the chemistry of the far-field waters, particularly with respect to redox conditions. Many radionuclides of concern (e.g. U, Np, Pu) are much less soluble (and therefore less mobile) at lower oxidation states ($+3, +4$) than at higher oxidation states ($+5$ and $+6$).

The water present in the bentonite buffer of a high-level nuclear waste site can be expected to be more reducing, and therefore, less conducive to radionuclide transport (particularly for Pu, Np and U), than the oxygenated glacial meltwaters that may intrude into the far-field environment sometime in the distant future (Glynn and Voss, 1999). The bentonite contains significant amounts of organic matter and pyrite, which provide it with a relatively strong reducing capacity. In the current Swedish design, the steel and copper present in the canisters planned to encapsulate the high-level waste can be expected to provide significant reducing capacity. Similarly, in low level and intermediate level nuclear waste-disposal sites, the presence of steel and iron barrels, and of detrital organic matter, such as

cardboard and paper products, should also generate reducing conditions in the near field. The distribution of redox conditions is likely to be quite heterogeneous. High organic carbon concentrations in the waste disposal areas may lead to significantly enriched pCO_2 values for the waters recharging through these areas. pH values may also differ markedly from values in the far-field environment. Higher dissolved carbonate concentrations in the recharging waters could significantly increase the aqueous stability, and mobility, of radionuclides such as Pu, Np, Am, and U.

The numerical simulations presented in the next section examine only a few of the geochemical uncertainties inherent in modeling the sorption, and retarded transport, of two radionuclides, neptunium (Np) and plutonium (Pu), in the Fennoscandian ground-water environment.

3. Pu and Np transport calculations

3.1. Simulation setup

One-dimensional simulations of Pu and Np transport were conducted using version 2.3 of the PHREEQC code (Parkhurst and Appelo, 1999) with thermodynamic data for Np and Pu aqueous species and minerals taken from the HATCHES database (version 11: NEA, 1999; Cross and Ewart, 1991) and data for Pu(IV), Pu(V) and Np(V) surface-complexation constants for goethite taken from Turner's (1995) compilation. No surface-complexation constants were available for Np(IV) sorption. The simulations also ignored radioactive decay of Pu and Np isotopes. Example PHREEQC input files used for the simulations can be downloaded by anonymous ftp to ftp.iamg.org. Simulation details and discussion are also available in Glynn (Glynn, 2003, draft SKI report).

Davis and Kent (1990), Dzombak and Morel, 1990, and Turner (1995) provide comprehensive descriptions of the diffuse double-layer surface-complexation sorption (DDLSC) model that is used in the simulations presented here. In the DDLSC model, a surface has a fixed number of sorption sites (referred to here as the "sorption capacity" and expressed in moles of sorption sites per kg of H_2O), but the charge on individual sites, and the charge of the entire surface, varies as a function of the pH and composition of the adjoining aqueous solution. At a given pH and composition, there generally is a distribution of positively charged, negatively charged, and neutrally charged sites on the surface. These sites can potentially sorb a variety of anionic, neutral or cationic aqueous species. The specific distribution of positive, negative, and neutral surface sites depends on the pH (and composition) of the adjoining solution. Aqueous species sorbed to the various surfaces sites are considered "surface complexes", and the speciation of the surface (into protonated, neutral and deprotonated sites) and its "surface complexes" is treated similarly, from a thermodynamic and mathematical point of view to an aqueous speciation calculation.

The 1D columns in the simulations presented here contained 100 cells, 5 m each in length, with 1 kg of H_2O in each cell. A time step of half a year was used, resulting in a simulated average linear velocity of 10 m per year and an advective transport time (for a chemically conservative constituent) of 50 years for the 500 m length of the column. This ground-water transport time corresponds to that expected during times of glacial advance and retreat at the Äspö site (Glynn and Voss, 1999; Geier, 1996). In addition to advection, PHREEQC also simulated longitudinal hydrodynamic dispersion through a centered-in-space finite-difference approximation. A fixed, arbitrary and uniform, longitudinal dispersivity coefficient α of 1 m was used throughout the column. This value of α is reasonable for transport in a fractured rock environment given the simulation scale (500 m).

The PHREEQC code simulated the following chemical equilibria, in each cell, at each time step in the transport simulations: (1) surface-complexation reactions between the advecting waters and an immobile goethite surface (with an arbitrarily chosen, 5×10^{-6} moles of sorption sites/kg H_2O initially on average, in each cell, or a total of 5×10^{-4} moles of sorption sites for the entire column), (2) pyrite and calcite dissolution/precipitation reactions, and (3) aqueous speciation and hydrolysis reactions. Initial pyrite and calcite concentrations of 10 moles/kg H_2O were sufficiently high that they never became depleted in any cell during the simulations.

3.1.1. "Infiltration" stage conditions

Each transport run consisted of two stages. In a first stage, CO_2- and O_2-rich glacial meltwater contaminated with Np and Pu infiltrated the column, displacing uncontaminated water (cf. Table 1) and mixing with it (as a result of the specified dispersivity of 1 m). The glacial meltwater also reacted in each cell with pyrite and calcite, and with a surface (with goethite sorption characteristics). Redox conditions, pH, ionic strength and other chemical characteristics of the aqueous solutions present in the column varied spatially and temporally as a result of the simulated chemical reactions, as a result of the mixing induced between cells and as a result of the advective "shifting" of the aqueous solutions from one cell to the next at each time step.

The infiltrating glacial meltwater (Glynn et al., 1999) was assumed to have a major ion composition typical of dilute glacial meltwaters and a temperature of $-1.8°C$,

Table 1
Chemical compositions of initial waters used for speciation, mass-transfer and mass-transport modeling

	Temp.	pH	pe^-	Ca	Mg	Na	K	Alk.	Cl	SO_4	Li	Fe	Si
Fjallsjökull glacial meltwater	−1.8	7	N/A	4.24	0.67	2.34	0.25	14.03	N/A	2.54	N/A	N/A	N/A
KASO2 (530–535 m)	15.2	8.1	−5.41	1890	42	2100	8.1	10	6410	560	1	0.244	4.1

Temperature is given in °C. Concentration units are mg/l. Nitrate is expressed as mg/l of N. Alkalinities are expressed as mg/l of HCO_3. 1.4×10^{-3} moles of O_2, 0.0257×10^{-3} moles of CO_2, 10^{-8} moles of Np and 10^{-8} moles Pu were added, per kg of water, to Fjallsjökull water prior to its infiltration into one-dimensional column (during first stage of transport simulations). N/A stands for data not available.

the estimated melting temperature of ice at the base of a 2 km high ice sheet. This temperature was chosen as a limiting case. The intruding water potentially could have a temperature closer to 6°C, by the time it becomes contaminated with Pu and Np, assuming this happens at a depth of near 500 m (discounting erosion of the present land surface), and assuming an invariant geothermal gradient. A change in infiltrating water temperature does not affect the conclusions of this paper (cf. Glynn, 2003, draft SKI report). Because there is almost no heat capacity information for Np and Pu species to allow extrapolation of the Np and Pu thermodynamic data (beyond 25°C standard state conditions), changing the temperature of the infiltrating water mainly affects the redox state and major ion chemistry of the waters, and only indirectly affects Np and Pu concentrations.

Similarly, the chemical characteristics of a subglacial meltwater were chosen as a limiting case. The composition, pH and redox characteristics of an infiltrating meltwater could change substantially as a result of reactions in the far-field and near-field environments, particularly if the water had to travel through 500 m of fractured rock environment before becoming contaminated with Pu and Np. It is possible that the glacial meltwaters could come into contact with Pu and Np sorbed or deposited well above a depth of 500 m, as a result of a previous contamination leak (perhaps during a previous glaciation). In this case, the chemical characteristics and temperature of the infiltrating waters could remain close to those of a subglacial meltwater. For the purpose of the scenario presented here, the Np and Pu contaminated glacial meltwaters have to travel 500 m before exiting the 1D column. This could correspond to a flow path traveling from a repository site to the surface (e.g. the upward flow section of a flow cell initiated by meltwater at the base of an accreting warm-based ice sheet), or it could correspond to a different hydrologic situation.

The chemical composition used for the infiltrating meltwater corresponds to that of water sampled from the Fjallsjökull Glacier in Iceland (Raiswell and Thomas, 1984). The dissolved CO_2 and O_2 concentrations (2.57×10^{-5} m and 1.4×10^{-3} m, respectively) added to the Fjallsjökull water are consistent with some of the lowest concentrations of trapped gases measured in ice from the base of the Greenland ice sheet (Stauffer et al., 1985). Actual gas concentrations could be twice as high. In simulations conducted for a performance assessment, conservatism could require using higher O_2 and CO_2 concentrations than those used in the present simulations. Upon melting of the ice at the bottom of a warm-based ice sheet, trapped air is expected to dissolve entirely because of the 2 km-high hydrostatic head, which is equivalent to a pressure of about 200 atmospheres.

Pu and Np concentrations of 10^{-8} molal were added to the glacial meltwater. Those concentrations are typical of the values considered for Pu and Np transport simulations "under oxidizing conditions" conducted for performance assessments of potential or analog high-level-nuclear-waste disposal sites in the Swedish Nuclear Waste program (e.g. SKI SITE-94, 1996). In the oxygenated glacial meltwater used here, PHREEQC calculations partition most (about 97%) of the Pu and Np added in the pentavalent oxidation state, with the remainder in the hexavalent state. As the infiltrating glacial meltwater disperses and reacts with pyrite and calcite (which never become depleted) and consequently becomes more reducing, Np(IV) and Pu(IV) oxidation states become the predominant oxidation states in the reacted water.

The background water initially present in the column corresponds to water sampled from the KAS02 borehole at 530 m depth under Äspö Island on the Baltic coast. It is typical of waters presently found at that depth along the Baltic coastline: low alkalinity, reducing, and predominantly rich in Na, Ca and Cl. The waters are intermediate in composition and salinity between the $NaHCO_3$ waters found near the ground surface and the $CaCl_2$ shield brines found at depths of a kilometer or more. The relatively high Ca concentrations (leached from calcic-silicate minerals) cause calcite precipitation, resulting in the low observed alkalinity. Mg is low relative to Ca and Na, possibly because of its uptake in chlorite. The small amount of dissolved organic matter, and its refractory nature, drives a slow process of sulfate reduction, generating sulfide. The sulfide precipitates out in the form of iron sulfide, usually embedded in

secondary calcite. Primary pyrite also is available in the rock matrix and in hydraulically disconnected or less conductive fractures. Glynn and Voss (1999) further describe the chemistry of ground waters near the Äspö HRL. Because of its representative nature, the water sampled from borehole KASO2 at 530 m depth was chosen as the "reference" water used for performance assessment calculations in the SKI SITE-94 project (SKI SITE-94, 1996).

The partitioning of Np and Pu between the infiltrating glacial meltwater and the background-water-equilibrated surface initially present in the simulation column was first calculated in a "batch" (i.e. no transport) PHREEQC calculation, that also included equilibration of the reacting water with pyrite and calcite. This simulation resulted in K_r partition coefficients of 45.7 for Pu and 0.318 for Np, corresponding to predicted retardation factors of 46.7 and 1.3, respectively for Pu and Np. (For comparison purposes, a similar batch calculation using the KAS02 water contaminated with 10^{-8} m Np and Pu and no calcite or pyrite equilibrium resulted in K_r partition coefficients of 289. for Pu and 2.39×10^{-4} for Np.)

The first transport stage, or "infiltration" stage, was run until the entire column was at steady state with respect to both Pu and Np (typically for up to 4000 years, i.e. 80 pore volumes). This first transport stage can be thought of as representing a model of Pu and Np transport, from a 500 m deep repository to the surface, after establishment of a Pu and Np leak in the near field (not considering near-field chemical effects) or it can represent any other scenario of progressive Pu and Np contamination.

3.1.2. "Cleanup" stage conditions

Subsequently, in a second stage of the transport simulations, the "cleanup" stage, the infiltrating solution was changed back to the uncontaminated reference water from the KAS02 borehole and the transport simulations were run until almost no Pu or Np was left in the column. The direction of flow was not changed, only the chemistry of the infiltrating water. The "cleanup" stage typically ran for up to 15,000 years (i.e. 300 pore volumes). The chemical and mineralogical conditions in the 500 m long 1D column at the beginning of the "cleanup" stage reflected the conditions in the column at the end of the "infiltration" stage.

A PHREEQC "batch" calculation of the Pu and Np desorption resulting from an equilibration between one cell volume of uncontaminated background (KAS02) water and a contaminated-meltwater-equilibrated surface resulted in K_r partition coefficients of 1920 for Pu and 6.67×10^{-3} for Np, i.e. in a high retardation factor for the movement of a potential Pu desorption front.

3.1.3. Investigation of chemical heterogeneity: setup of sorption capacity distributions

The initial distribution of sorption capacities was changed in different transport runs. A first transport run used a uniform column, with initially identical sorption capacities in each cell. Four other transport runs used a random log-normal distribution of sorption capacities. The random distribution was created with the ran1 function documented by Press et al. (1992, p. 271). In all transport runs, the initial column always had the same average and total sorption capacities as in the uniform column case.

Sorption capacity distributions with standard deviations (σ) of 0.5, 1 and 2 log units (chosen arbitrarily) were used in three transport runs. In these three runs, the spatial distribution of the sorption capacities was identical (i.e. were based on a single random distribution), the only difference being that the capacities themselves were proportionally scaled so as to obtain the desired standard deviation. Finally, a fifth transport run used the same distribution of sorption capacities previously used for the $\sigma = 1$ case, but with a different spatial arrangement so that the sequence had an autocorrelation length λ of close to 8 m (almost 2 cell lengths) rather than 2 m (the initial case). In other words, the series of sorption capacity numbers used in this run was the same as that for the $\sigma = 1$ case, except that the numbers were manually placed in a different spatial order. Autocorrelation lengths were calculated as in Domenico and Schwartz (1998, p. 229).

3.2. Pu and Np transport: "infiltration" stage results

Results obtained for the "infiltration" stage of the PHREEQC simulations show that an equivalent retardation factor of about 40 is obtained for Pu transport, in the case of the uniform column (cf. Pu profiles in Fig. 3). It takes about 40 pore volumes (2000 years) for the Pu front to reach the end of the 500 m column. This compares favorably with the K_r ratio of 45.7, corresponding to a retardation factor of 46.7, previously obtained in the PHREEQC batch simulation. As the standard deviation of the log-normal distribution of the sorption capacities is increased, from $\sigma = 0$, to 0.5, to 1 and finally to $\sigma = 2$ log units, the spread of the Pu infiltration front becomes greater, meaning that low Pu concentrations reach the end of the column sooner, but that a significant mass of Pu also stays further behind (particularly near 300 m, where several cells with high sorption capacities are located, a result of the random distribution), thereby delaying attainment of steady-state conditions in the column (Fig. 3). Results obtained for the column with the spatially redistributed sorption capacities ($\lambda = 8$ m) differ very little from results obtained for the original column ($\lambda = 2$ m) with the same standard deviation ($\sigma = 1$ log units).

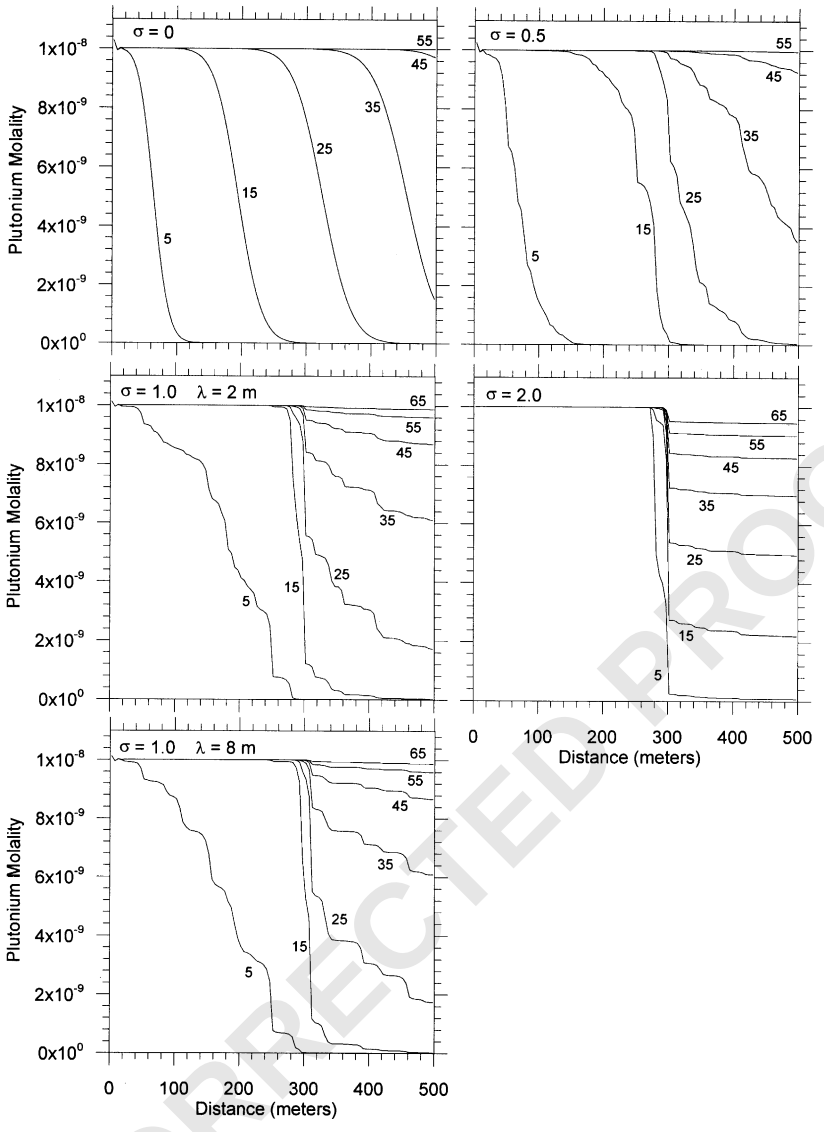

Fig. 3. Plutonium infiltration as function of distance for five different sorption capacity distributions. Number of pore volumes (50 yr per pore volume) is indicated for each curve.

The Np transport results differ from the Pu results in that Np transport shows little retardation (Fig. 4), as already predicted by the PHREEQC batch simulation (K_r Np = 0.32 or $R = 1.32$). Little more than a pore volume is required for the Np to infiltrate throughout most of the column. A mid-concentration of 5×10^{-9} molal Np is reached at the end of the column before 1.5 pore volumes (75 years). Nevertheless, despite the almost conservative behavior of Np, the profile curves do not exhibit a simple Gaussian shape, even in the case of the uniform column. The profiles obtained for the non-uniform columns reflect the higher sorption capacities present near 300 m, and a resulting trough in aqueous Np concentrations at that location.

The Pu breakthrough curves obtained at the end of the columns are much smoother than the profile curves displayed in Fig. 3: the breakthrough curves (Fig. 5) spatially integrate the distribution of sorption capacities over the entire column. Despite an identical *total* sorption capacity for each of the five columns, greater spreading of the breakthrough curves is obtained for sorption capacity distributions with higher standard deviations. These results appear similar to those that might be obtained as a result of increasing the longitudinal dispersivity in a transport simulation using a linear isotherm approach (constant K_d), except that the breakthrough curves here are perhaps more asymmetrical. The curves show a tailing effect and also cross

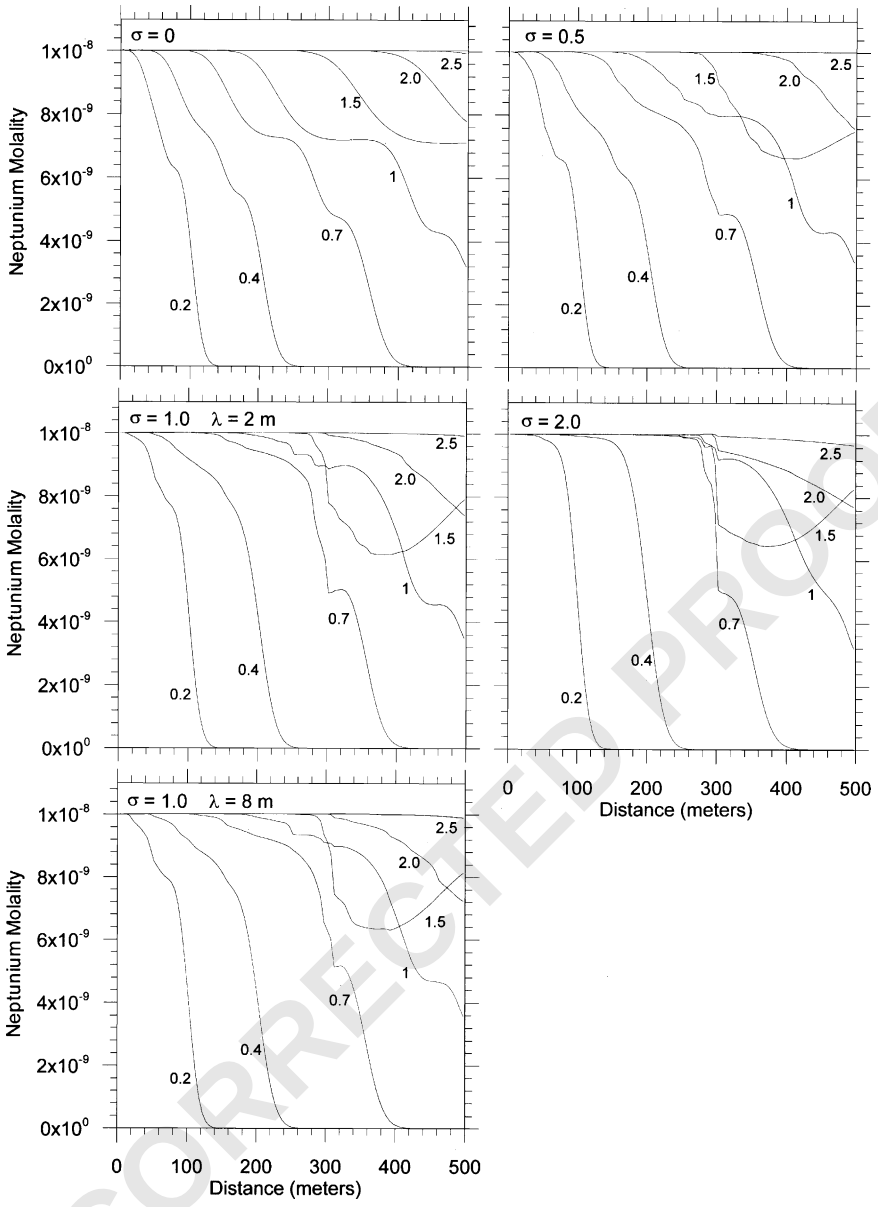

Fig. 4. Neptunium infiltration as function of distance for five different sorption capacity distributions. Number of pore volumes (50 yr per pore volume) is indicated for each curve.

each other near a concentration of 8×10^{-9} molal rather than at a mid-point of 5×10^{-9} molal, which would be expected in the case of a linear sorption isotherm. These observations were confirmed by fitting the PHREEQC-simulated Pu breakthrough curves with the CXTFIT code (Toride et al., 1999). In addition to many other capabilities, CXTFIT can fit concentration versus time data using an analytical solution to the advection–dispersion equation with constant retardation. The fit results (Table 2; Fig. 6) document an exponential increase in the fitted "apparent" dispersivity (from 1.8 to 122 m) as a function of an increasing spread in the distribution of sorption capacities (from $\sigma = 0$ to 2 log units). The results also document an accompanying, almost linear, decrease in the fitted "apparent" retardation factors, from a value of 38 ($\sigma = 0$) down to a value of 24 ($\sigma = 2$).

The Np breakthrough curves (Fig. 7) obtained at the end of the columns differ from the ones obtained for Pu. Despite the much more conservative behavior of Np compared to Pu, Np transport differs considerably from that of a truly conservative constituent. Indeed,

although the leading Np front crosses the end of the column after 50 years, the Np concentrations actually dip downwards soon after, before rising again to the steady-state concentration of 10^{-8} molal. This behavior is caused by differences in the extent of Np sorption that naturally arise during the transport simulations, as a result of the reequilibration of the surface present in each cell with waters of varying chemical characteristics. The extent of the "dip" increases with an increasing spread in the distribution of the sorption capacities, although the results obtained for the $\sigma = 2$ column are close to those obtained for the $\sigma = 1$ column. Arrival times of the concentration peaks and troughs are similar in all cases. The Np breakthrough curves differ markedly from the curves that would be obtained for a simulation of the advection dispersion equation with constant K_d and, therefore, fitting with CXTFIT was not attempted.

3.3. Pu and Np transport: "cleanup" stage results

The Pu and Np transport results obtained during the "cleanup" stage show that a Pu and Np rich spike is desorbed from the Np- and Pu-saturated goethite surface as a result of the infiltration of the initially uncontaminated reference water used to "cleanup" the column. The desorption spike persists as it moves into the column because potential sorption sites in down-gradient cells already contain high sorbed Np and Pu concentrations. The spike moves through the column unretarded, or actually, slightly faster (because of hydrodynamic dispersion and reaction) than it would

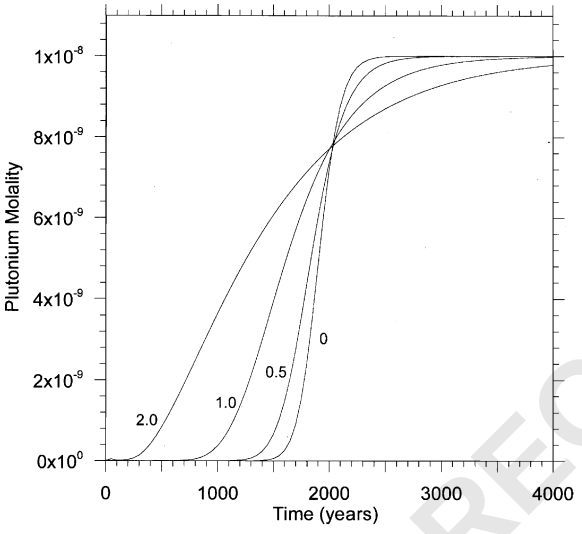

Fig. 5. Pu concentrations obtained as function of time at end of 500 m long column, during "infiltration" stage of PHREEQC transport simulations. Four curves plotted correspond to sorption capacity distributions with different standard deviations (uniform or 0, 0.5, 1, and 2 log units).

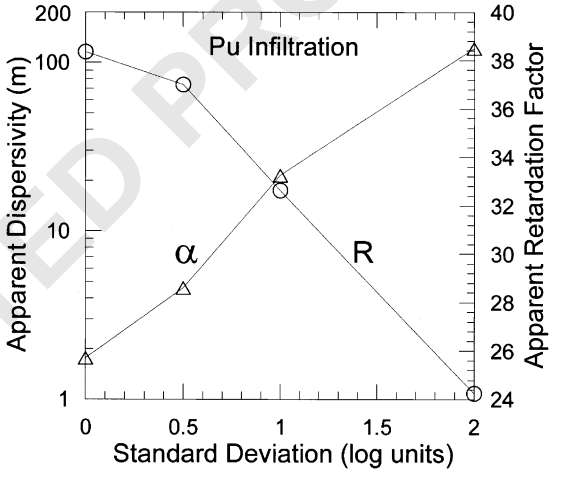

Fig. 6. Dispersivity and retardation factor fitting results obtained applying the CXTFIT analytical solution code to Pu "infiltration" stage breakthrough curves (calculated with PHREEQC code) as function of standard deviation of sorption capacity distribution.

Table 2
Fitting results, obtained with the CXTFIT code, for Pu breakthrough curves (at end of 500 m column) obtained during "infiltration" stage of PHREEQC simulations

Column	Apparent dispersivity, α				Apparent retardation, R			
	α	S.E.	Low	High	R	S.E.	Low	High
$\sigma = 0$	1.76	0.01	1.74	1.78	38.3	0.007	38.3	38.4
$\sigma = 0.5$	4.58	0.03	4.53	4.64	37.0	0.011	37.0	37.0
$\sigma = 1$	21.4	0.20	21.0	21.8	32.6	0.030	32.6	32.7
$\sigma = 2$	122	1.19	119.	124.	24.2	0.052	24.1	24.4

Results are given for each of four columns with different sorption-capacity standard deviations. Fitted dispersivity, α, is expressed in meters. Standard errors (S.E.) of fitted parameters (α and R) are provided along with lower and upper bounds of 95% confidence limits.

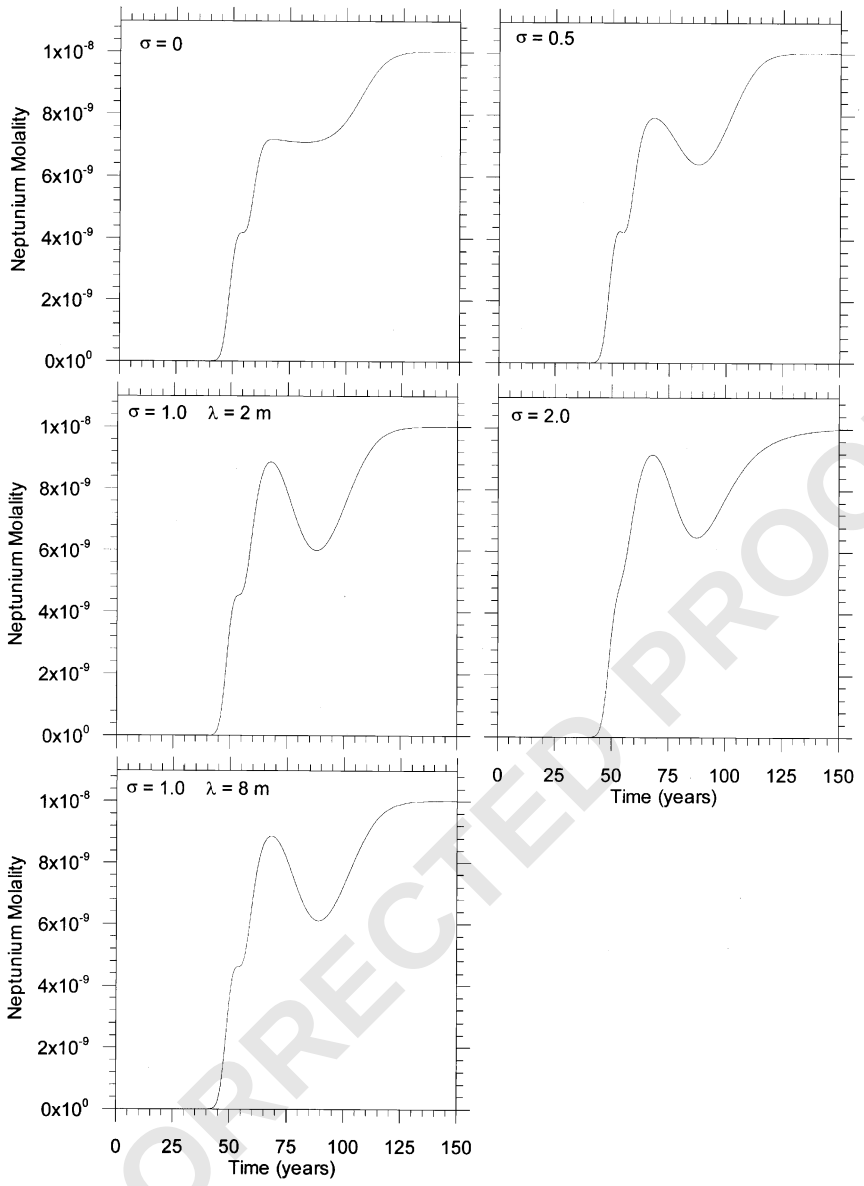

Fig. 7. Np concentrations as function of time at end of 500 m long column, during the "infiltration" stage of PHREEQC transport simulations.

through an advection-only process: it reaches the end of the column slightly before 1 pore volume (50 years). The Pu spike (Fig. 8) reaches a maximum concentration of close to 9×10^{-8} molal, *nine times higher* than the initial concentration present in the contaminated glacial meltwater. In contrast, the Np spike (Fig. 9) reaches a maximum concentration of only 2.5×10^{-8} molal, still 2.5 times higher than the initial concentration present in the contaminated glacial meltwater. Results for both radionuclides show a general decrease in maximum spike concentrations, with an increasing spread of sorption capacity distributions. The height of the spikes also varies with distance along the column. The spikes generally seem to increase in column areas where the sorption capacities are greater (near and after 300 m), particularly in the case of the column with the highest sorption capacity spread ($\sigma = 2$). Finally, the evolution of the Np spikes along the columns differs from that of the Pu spikes. For example, in the case of the uniform column ($\sigma = 0$), the Pu spike maintains a constant maximum concentration with distance, whereas the Np spike increases in magnitude as it travels along the column. Furthermore, the evolution of the radionuclides also differs in that the Np concentrations decrease to 0,

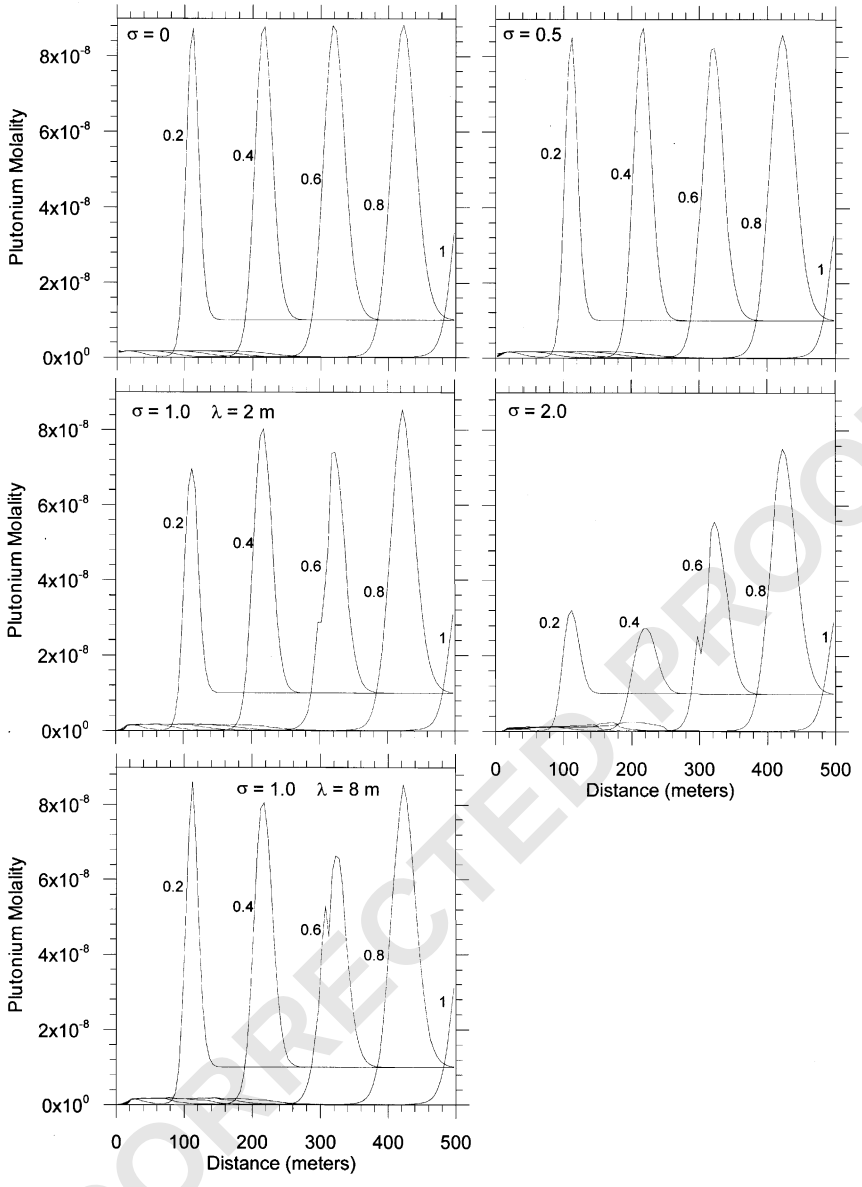

Fig. 8. Plutonium early "cleanup" profiles as function of distance for five different sorption capacity distributions. Number of pore volumes (50 yr per pore volume) is indicated for each curve.

upgradient of the Np spike (as expected for relatively conservative transport), whereas the Pu concentrations decrease drastically but then slightly increase to a value on the order of 10^{-9} molal.

The remaining Pu takes a long time to desorb and advect out of the column, more than 15,000 years (300 pore volumes) in the case of the non-uniform columns (Figs. 10 and 11). The aqueous Pu concentrations are as high as 1.7×10^{-9} molal, but decrease with an increasing spread of the sorption capacity distribution and an increasing number of pore volumes. In the case of the uniform column, the long-term Pu desorption front takes about 200 pore volumes (10,000 years) to advect out of the column, which is 5 times slower than the movement of the Pu front during the "infiltration" stage of the transport simulation. This result indicates that Pu sorption, like that of many other sorbing contaminants, is considerably stronger at lower aqueous concentrations, and, consequently, does not follow the constant K_d model often used in contaminant transport codes. None of the "cleanup" stage simulation results obtained and discussed above could ever be duplicated by a linear sorption (constant K_d) or even by a Freundlich sorption model, without, at a minimum, changing the values of

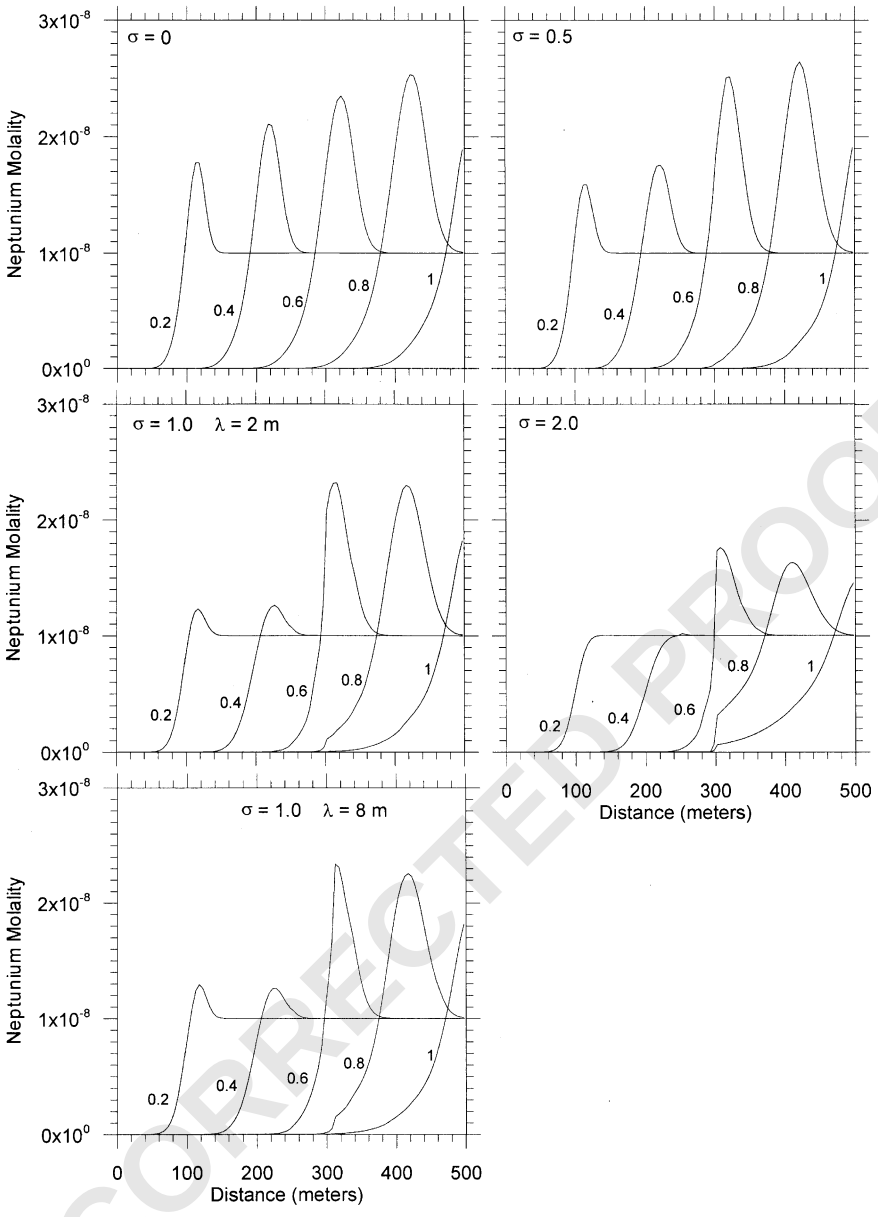

Fig. 9. Neptunium "cleanup" profiles as function of distance for five different sorption capacity distributions. Number of pore volumes (50 yr per pore volume) is indicated for each curve.

the model constants as a function of both time and distance. Use of a two-site sorption surface complexation model (containing both "weak" and "strong" sorption sites as often used for hydrous ferric oxide surfaces) would have accentuated the non-linear sorption behavior observed in the simulations presented here. Lack of "strong-site" thermodynamic complexation data for Pu and Np precluded the use of a two-site model.

The effect of changing the spread of the distribution of sorption capacities on the cleanup of Pu in the 500 m column is best illustrated by the breakthrough curves obtained for the Pu late "cleanup" at the end of the column (Fig. 11). As can be seen in Fig. 11, an increasing spread (from $\sigma = 0$ to 2) has the effect of lowering the Pu concentrations coming out of the column, but by doing so increases the time required to completely clean the column. Changing the spatial distribution of the sorption capacities, i.e. the autocorrelation length λ, for the $\sigma = 1$ case does not affect the results in any measurable way (and, therefore, the results are not plotted on Fig. 11).

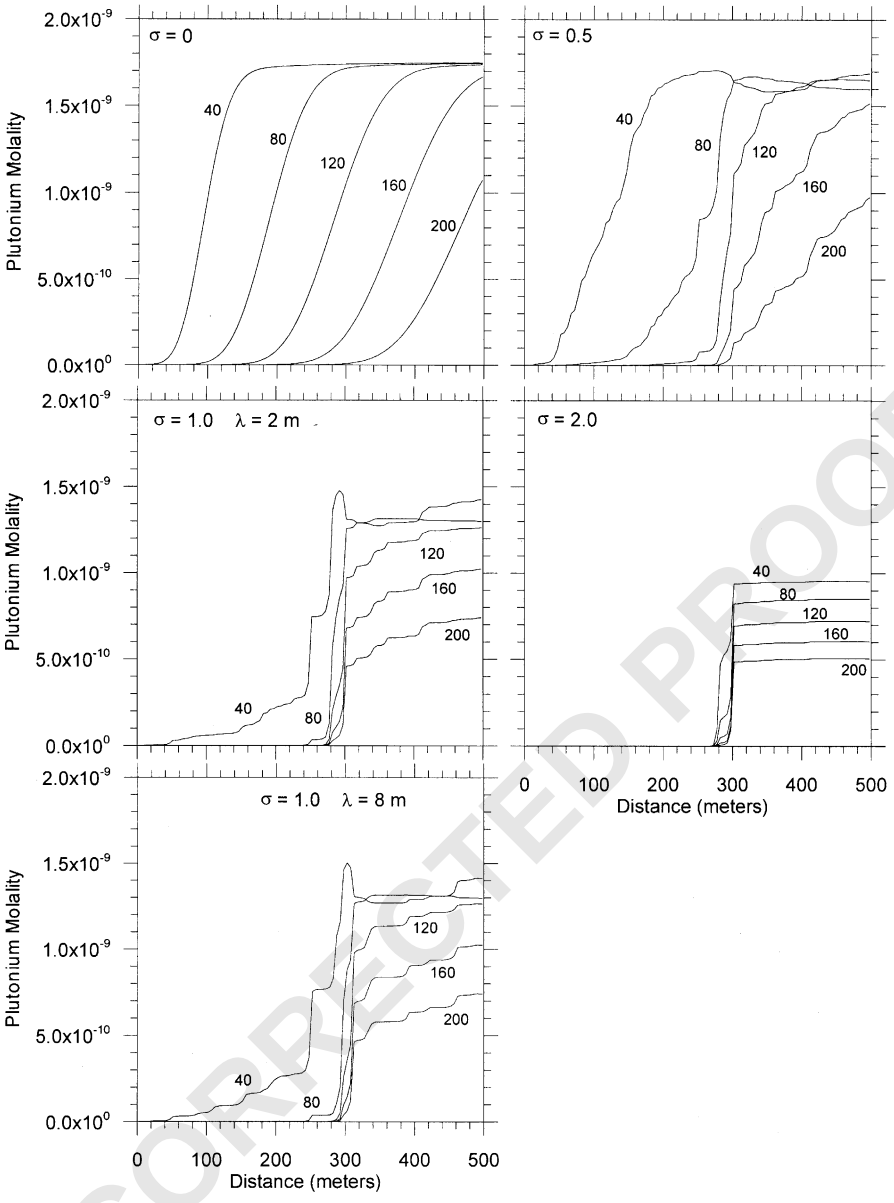

Fig 10. Pu late "cleanup" profiles. Number of pore volumes (50 yr per pore volume) is indicated for each curve.

The PHREEQC-simulated Pu breakthrough curves obtained during the late "cleanup" stage simulations were fitted with the CXTFIT code (Toride et al., 1999). The fits obtained (Table 3; Fig. 12) show higher "apparent" longitudinal dispersivity and retardation factor values, but similar trends to the fits obtained for the Pu "infiltration" breakthrough curves. The fits again document an exponential increase in the fitted "apparent" dispersivity (from 6.6 to 277 m) as a function of an increasing spread in the distribution of sorption capacities (from $\sigma = 0$ to 2 log units), and an accompanying decrease in the fitted "apparent" retardation factors, from a value of 210 ($\sigma = 0$) down to a value of 184 ($\sigma = 2$). In general, the fits are not as good as those obtained for the "infiltration" stage breakthrough curves. This is particularly true for the $\sigma = 1$ case.

4. Conclusions

The advantages and limitations of empirical approaches, such as the K_d, Langmuir and Freundlich

models, to sorption modeling were discussed and contrasted to those of thermodynamic surface-complexation models. Some common uncertainties affecting sorption and contaminant transport modeling are highlighted in this paper. These uncertainties are present: (1) in the conceptual model of processes controlling contaminant sorption, (2) in the thermodynamic and/or the empirical description of those processes, (3) in the description of present-day field environments and (4) in the description of the evolution of those environments. The simulations presented in this paper address only a few of the many uncertainties involved in reactive transport modeling.

Through 1D reactive transport simulations that considered competitive ion-exchange reactions between ^{90}Sr, Ca, Na, Mg and K and the kinetically limited dissolution of calcite, Reardon (1981) determined that the partitioning of ^{90}Sr varied as a function of both space and time. He consequently argued against the use of the constant K_d approach in reactive transport models. Although the present study agrees with Reardon's (1981) findings concerning the general limitations of the K_d approach, Reardon (1981) would have obtained a spatially constant ^{90}Sr partition coefficient under steady-state conditions, and would have obtained a near-constant retardation factor for the movement of his simulated ^{90}Sr front, had he assumed local equilibrium for all the reactions considered in his initially uniform composition column.

The PHREEQC 1D Pu and Np transport simulations presented here provide examples of some of the functional limitations of empirical sorption models, the constant K_d model in particular, but also others such as

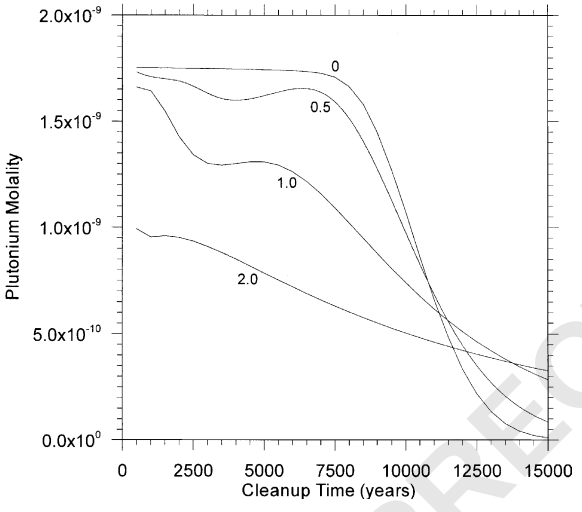

Fig. 11. Breakthrough curve (at end of 500 m column) for long-term "cleanup" of Pu. Four curves plotted correspond to sorption capacity distributions with different standard deviations (uniform or 0, 0.5, 1, and 2 log units).

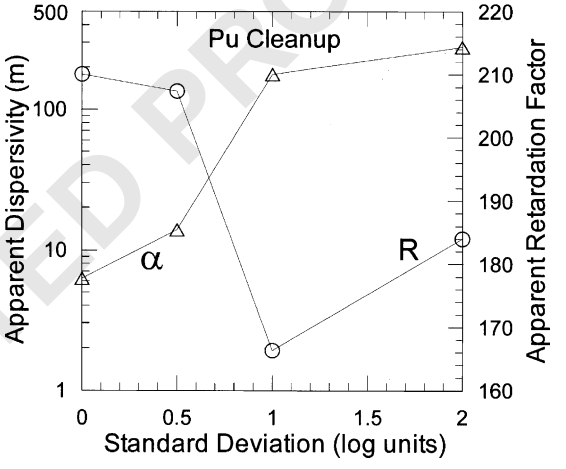

Fig. 12. Dispersivity and retardation factor fitting results obtained applying CXTFIT analytical solution code to Pu "cleanup" stage breakthrough curves (calculated with PHREEQC code) as function of standard deviation of sorption capacity distribution.

Table 3
Fitting results, obtained with CXTFIT code, for Pu breakthrough curves (at end of 500 m column) obtained during "cleanup" stage of PHREEQC simulations

Column	Apparent dispersivity, α				Apparent retardation, R			
	α	S.E.	Low	High	R	S.E.	Low	High
$\sigma = 0$	6.26	0.09	6.07	6.45	210	0.173	210	210
$\sigma = 0.5$	13.8	0.43	13.0	14.7	207	0.498	206	208
$\sigma = 1$	177	35.1	105	249	166	5.79	154	178
$\sigma = 2$	277	8.51	260	295	184	1.00	182	186

Results are given for each of four columns with different sorption-capacity standard deviations. Fitted dispersivity, α, is expressed in meters. Standard errors (S.E.) of fitted parameters (α and R) are provided along with lower and upper bounds of 95% confidence limits.

the Freundlich and Langmuir sorption models. In the present simulations, sorption was assumed the predominant retardation process controlling Pu and Np transport, and was modeled using a diffuse-double-layer-surface-complexation (DDLSC) model. Local equilibrium was assumed for all reactions. The infiltration of Np- and Pu-contaminated waters into an initially uncontaminated environment was simulated first, until uniform aqueous concentrations of Np and Pu were obtained through the 500 m long column. A second stage simulated the cleanup of Np and Pu from the column as uncontaminated water seeped back into the column. Simulations were conducted using columns with different sorption capacity distributions: with the same total sorption capacity, but with different extents of variance. A single, spatially random, log-normal distribution of the sorption capacities was used for most of the non-uniform columns, with sorption capacity values appropriately scaled so as to obtain different standard deviations. The effect of changing the spatial correlation structure, by doubling the autocorrelation length, was also tested in a separate simulation, but results obtained were not significantly affected by the change.

The primary findings of the PHREEQC simulations presented here are:

1. Pu and Np partitioning coefficients, and associated retardation factors, varied non-linearly with increasing concentration, although close to constant values were obtained in the case of a spatially uniform distribution of sorption capacities.
2. Effective partitioning coefficients describing radionuclide transport (by desorption) during the "cleanup" stage markedly differed from values applicable to transport during the "infiltration" stage. The retardation factors for Pu cleanup were five to six times greater than those obtained for Pu infiltration in the various columns.
3. Np and Pu aqueous concentrations obtained during the "cleanup" stage were as much as nine times greater than concentrations initially present in the Np/Pu contaminated waters. Commonly used empirical sorption models, such as the K_d, Langmuir and Freundlich models, could not have predicted the high concentration spikes.
4. Increasing the variance of the sorption capacity distribution resulted in a marked increase in the spreading of the breakthrough curves for Pu, a strongly sorbed constituent, and mimicked the effect of an exponential increase in longitudinal dispersivity. A fit of the breakthrough curves, using the CXTFIT code simulating the standard advection–dispersion equation with a constant K_d, showed that the increase in the fitted dispersivities was also accompanied by a significant decrease in the fitted retardation factors.
5. Despite weak sorption and almost insignificant retardation (under the geochemical conditions used in the simulations), Np concentration profiles and breakthrough curves exhibited trend reversals and complex transport behavior. Commonly used empirical sorption models could not have predicted this behavior. Such behavior observed for an almost conservative constituent, under 1D, homogeneous flow conditions, suggests caution should be used in interpreting short-term monitoring trends observed in ground-water contamination cases or field tracer tests.
6. The simulations conducted here considered complexity and variance for only a few chemical and mineralogical effects. Additional simulations have been conducted that document the effects (on Np and Pu migration) of changing (1) the background mineral assemblage, (2) the infiltrating water temperature, (3) the infiltrating water chemistry, (4) of using different Np and Pu concentrations in the infiltrating water, (5) of using a different thermodynamic database for aqueous Np and Pu species, and (6) a different specific surface area. These results, which further examine non-linear sorption behavior, are documented in an SKI report (Glynn, 2003, draft SKI report).
7. Although the results presented here illustrate complex non-linear behavior, even greater functional complexity would have been obtained if factors such as varying reaction kinetics, physical heterogeneity and 3D effects had been taken into consideration. Planned future work will consider some of these other effects.
8. Transport simulations conducted using the DDLSC and other multi-species competitive sorption models may provide guidance in the appropriate use of simpler sorption models, and may help in making minimum and maximum estimates of radionuclide retardation, if adequate thermodynamic and kinetic reaction data are available.

Acknowledgements

I thank Robbie Greene for his help in running and extracting the results of the simulations presented in this paper. I am also very grateful for the detailed reviews provided by Eric Reardon, Bo Strömberg, Dave Turner and an anonymous reviewer; they significantly improved the paper. This work was funded by the US Geological Survey and the Swedish Nuclear Power Inspectorate (SKI).

References

Cross, J.E., Ewart, F.T., 1991. Hatches—a thermodynamic database and management system. Radiochimica Acta 52/53, 421–422.

Davis, J.A., Kent, D.B., 1990. Surface complexation modeling in aqueous geochemistry. In: Hochella, M.F., White, A.F. (Eds.), Mineral–Water Interface Geochemistry. Mineralogical Society of America. Reviews in Mineralogy 23, 177–260.

Davis, J.A., Coston, J.A., Kent, D.B., Fuller, C.C., 1998. Application of the surface complexation concept to complex mineral assemblages. Environmental Science and Technology 32 (19), 2820–2828.

Domenico, P.A., Schwartz, F.W., 1998. Physical and Chemical Hydrogeology, 2nd Edition, Wiley, New York, NY, 506pp.

Dzombak, D.A., Morel, F.M.M., 1990. Surface Complexation Modeling: Hydrous Ferric Oxide. Wiley, New York, NY, 393pp.

Geier, J., 1996. Discrete-feature modeling of the Äspö site: 3. Predictions of hydrological parameters for performance assessment. SKI (Swedish Nuclear Power Inspectorate), SKI Report 96:7, 211pp.

Glynn, P.D., 2003. Plutonium and neptunium transport: sorption modeling for performance assessment of nuclear waste disposal in the Ferro scandian shield. Draft Report, Swedish Nuclear Power Inspectorate (SKI).

Glynn, P.D., Brown, J.G., 1996. Reactive transport modeling of acidic metal-contaminated ground water at a site with sparse spatial information. In: Steefel, C.I., Lichtner, P., Oelkers, E. (Eds.), Reactive Transport in Porous Media: General Principles and Application to Geochemical Processes. Mineralogical Society of America, Reviews in Mineralogy 34, 377–438.

Glynn, P.D., Voss, C.I., 1999. Geochemical characterization of Simpevarp ground waters near the Äspö Hard Rock Laboratory. SKI (Swedish Nuclear Power Inspectorate). SKI Report 96:29, 210pp.

Glynn, P.D., Engesgaard, P., Kipp, K.L., 1991. Use and limitations of two computer codes for simulating geochemical mass transport at the Pinal Creek toxic-waste site. In: Mallard, G.E., Aronson, D.A. (Eds.), USGS Toxics Substances in Hydrology Program, Proceedings of the Technical Meeting, Monterey, CA, March 11–15, 1991. US Geological Survey Water Resources Investigation Report 91-4034, pp. 454–460.

Glynn, P.D., Voss, C.I., Provost, A.M., 1999. Deep penetration of oxygenated meltwaters from warm based ice sheets into the Fennoscandian shield. In: Use of Hydrogeochemical Information in Testing Groundwater Flow Models, Technical Summary and Proceedings of a Workshop, Borgholm, Sweden, September 1–3, 1997. Nuclear Energy Agency, Organization of Economically Developed Countries, pp. 201–241.

NEA, 1999. NEA-1210 ZZ-HATCHES-11: version 11 of the HATCHES thermodynamic database distributed by the US Dept. of Energy and the Nuclear Energy Agency (NEA) of the Organization of Economically Developed Countries (OECD).

Parkhurst, D.L., Appelo, C.A.J., 1999. User's guide to PHREEQC (version 2)—A computer program for speciation, reaction-path, 1D transport, and inverse geochemical calculations. US Geological Survey Water-Resources Investigations Report 99-4259, 312pp.

Press, W.H., Teukolsky, S.A., Vetterling, W.T., Flannery, B.P., 1992. Numerical Recipes in FORTRAN: The Art of Scientific Computing, 2nd Edition, Cambridge University Press, Cambridge, UK, 963pp.

Raiswell, R., Thomas, A.G., 1984. Solute acquisition in glacial melt waters. I. Fjallsjökull (Southeast Iceland): bulk melt waters with closed-system characteristics. Journal of Glaciology 30 (104), 35–43.

Reardon, E.J., 1981. Kd's—Can they be used to describe reversible ion sorption reactions in contaminant transport? Ground Water 19, 279–286.

SKI SITE-94, 1996. SKI SITE-94: Deep Repository Performance Assessment Project. Swedish Nuclear Power Inspectorate (SKI), SKI report 96:36, Vols. 1 and 2, 660pp.

Stauffer, B, Neftel, A., Oeschger, H., Schwander, J., 1985. CO_2 concentration in air extracted from Greenland ice samples. In: Langway, C.C., Oeschger, H., Dansgaard, W. (Eds.), Greenland Ice Core: Geophysics, Geochemistry and the Environment. Geophysical Monograph, American Geophysical Union 33, 85–89.

Toride, N., Leij, F.J., van Genuchten, M.Th., 1999. The CXTFIT code for estimating transport parameters from laboratory or field tracer experiments. US Salinity Laboratory, Agricultural research Service, US Dept. of Agriculture, Riverside CA, Research Report No. 137.

Turner, D.R., 1995. A uniform approach to surface complexation modeling of radionuclide sorption, Center for Nuclear Waste Regulatory Analyses, Report CNWRA 95-001.